Urolithiasis (2019) 47:125–135
https://doi.org/10.1007/s00240-018-1048-8

ORIGINAL PAPER

Calcifying nanoparticles induce cytotoxicity mediated by ROS-JNK signaling pathways

Jihua Wu[1] · Zhiwei Tao[1] · Yaoliang Deng[1,2] · Quan Liu[1] · Yunlong Liu[1] · Xiaofeng Guan[1] · Xiang wang[1]

Received: 28 March 2017 / Accepted: 19 February 2018 / Published online: 6 March 2018

Abstract

Calcifying nanoparticles (CNPs) play an important role in kidney stone formation, but the mechanism(s) are unclear. CNPs were isolated and cultured from midstream urine of patients with kidney stones. CNP morphology and characteristics were examined by electron microscopy and electrophoresis analysis. Chemical composition was analyzed using energy-dispersive X-ray microanalysis and Western blotting. Human renal proximal convoluted tubule cell (HK-2) cultures were exposed to CNPs for 0, 12 and 72 h, and production of reactive oxygen species (ROS), mitochondrial membrane potential and apoptosis levels were evaluated. CNPs isolated from patients showed classical morphology, the size range of CNPs were 15–500 nm and negative charge; they were found to contain fetuin-A. Exposure of HK-2 cells to CNPs induced ROS production, decreased mitochondrial membrane potential and decreased cell viability. Transmission electron microscopy showed that CNPs can enter the cell by phagocytosis, and micrographs revealed signs of apoptosis and autophagy. CNPs increased the proportion of apoptotic cells, down-regulated Bcl-2 expression and up-regulated Bax expression. CNPs also up-regulated expression of LC3-B, Beclin-1and p-JNK.CNPs are phagocytosed by HK-2 cells, leading to autophagy, apoptosis and ROS production, in part through activation of JNK signaling pathways. ROS and JNK pathways may contribute to CNP-induced cell injury and kidney stone formation.

Keywords Calcifying nanoparticles · Cytotoxicity · HK-2 cells · Kidney stone · ROS

Introduction

Kidney stones are a frequent disease in urology, and incidence continues to increase. Despite advances in kidney stone diagnosis and treatment, how they form continues to remain unclear. Although renal calculi can be cured in most cases, rates of morbidity were 7.45% in mainland China [1] and ranged from 0.1 to 14.8% in Western countries [2].The rates of recurrence are high more than 50% [3], highlighting a need to understand their etiology.

Many factors appear to influence kidney stone formation, including heredity, environment, metabolism, and the presence of microorganisms. While the initial site of calculus formation may be in the calcified plaques of the renal papilla [4], what causes formation of calcified plaques in the first place is unclear. Calcified nanoparticles (CNPs), which are also called "nanobacteria," "nanobacteria-like particles," "nanons," or "mineral-protein nanoparticles". It was discovered and named for the first time during cell culture by Kajander [5], CNPs exists in many human tissues, 50–500 nm in diameter, spherical or oval, with central cavity and heat-resistant apatite mineralized crust. It can proliferate and replicate by cultured in vitro. CNPs were considered biotic by some but abiotic by others, it was called "nanobacteria" or "nanobacteria-like structures" in the previous article due to the self-proliferation [6, 7], but recent studies have shown that CNPs is merely a mineral-protein nanoparticles with biomimetic functions [8]. But no matter what it is, CNPs are closely associated with ectopic

Jihua Wu and Zhiwei Tao Equal contributors and co-first authors.

✉ Yaoliang Deng
dylkf317@163.com

✉ Xiang wang
15182449@qq.com

[1] Department of Urology, The First Affiliated Hospital of Guangxi Medical University, Nanning 530021, Guangxi, China

[2] Department of Urology, The Langdong Hospital of Guangxi Medical University, Nanning 530021, Guangxi, China

calcification diseases and may contribute to kidney stone formation. CNPs have been found in the Randall's plaque [9], and they are cytotoxic to 3T6 fibroblasts or tumor cells in vitro [5, 10, 11].In addition, Wong et al [12] showed that mineralo-organic nanoparticles form human kidney diseases and thought that the nanoparticles were the possible cause for kidney stones. It suggests that CNPs may contribute to the renal tubular epithelial cell injury linked to kidney stone formation [13].

Here we explored potential mechanism(s) by which CNPs may participate in kidney stone formation. We examined CNPs in situ in patient tissues, and we exposed HK-2 human proximal tubule epithelial cells to CNPs isolated from patients with kidney stones.

Methods

Cell culture

HK-2 cells were purchased from the American Type Culture Collection (Manassas, VA, USA) and cultured in DMEM-F12 medium (Gibco, Life Technologies, Carlsbad, CA, USA) supplemented with 10% fetal bovine serum (FBS; Gibco). Cultures were incubated at 37 °C in an atmosphere of 5% CO_2.

CNP culture

Midstream urine was collected from patients with renal calculi and sterile-filtered (0.45 μm). Filtrate (1 ml) was cultured in RPMI 1640 medium containing 10% FBS at 37 °C in an atmosphere of 5% CO_2. The medium was replaced once every 2 weeks. CNPs were collected after 6 weeks.CNP concentration was adjusted to 2.0 Meclary turbidity (MCF) immediately before use.

CNP characterization

CNP morphology and internal structure were observed using transmission electron microscopy (H7650, Hitachi, Tokyo, Japan) and scanning electron microscopy (S3400, Hitachi). Elemental composition of CNPs was determined using energy-dispersive X-ray microanalysis. CNP size and zeta potential were analyzed using electrophoresis analysis (Zetaview, Particle Metrix, Germany). CNPs were demineralized using 0.6 N HCl, then analyzed by Western blotting for the presence of fetuin-A.

CNP cytotoxicity

HK-2 cells were seeded into 96-well plates at a density of 1×10^4 cells/well (100 μl/well) and cultured overnight at 37 °C in an atmosphere of 5% CO_2. Then cultures were exposed to CNPs (2 Meclary turbidity MCF) for 0, 12 and 72 h, cell viability was measured using the Cell Counting Kit-8 (CCK-8; Beyotime Biotechnology, Shanghai, China). CCK-8 solution (10 μl) was added to each well, plates were incubated for approximately 4 h, and then optical density (OD) at 450 nm was measured using a microplate spectrophotometer.

$$\text{Cell viability (\%)} = \text{Average OD}_{\text{sample}} / \text{Average OD}_{\text{control}} \times 100\ \%.$$

ROS production assay

HK-2 cells were seeded in 6-well plates (1×10^5 cells/well), incubated for 24 h, then exposed to CNPs (2 MCF) for 0, 12 and 72 h. Levels of intracellular ROS were determined using the Reactive Oxygen Species Assay Kit (DCFH-DA, Beyotime Biotechnology, Hangzhou, China). DCFH-DA diluent (10 mol/l, 1 ml) was added to wells, plates were incubated for 30 min at 37 °C, and cells were analyzed using flow cytometry (BD Biosciences, San Jose, CA, USA).

Mitochondrial membrane potential analysis

HK-2 cells were plated into 6-well dishes and exposed to CNPs (2 MCF) for 0, 12 and 72 h. Then mitochondrial membrane potential was assayed using a commercial kit (JC-1, Beyotime Biotechnology). JC-1 working solution (0.5 ml) was added to the cells, the dishes were incubated for 20 min at 37 °C, and the suspensions were analyzed by flow cytometry. Changes in mitochondrial membrane potential were determined based on changes in the ratio of red to green fluorescence emission. A reduction in this ratio suggests early apoptosis.

Apoptosis assay

HK-2 cells were plated into 6-well dishes (1×10^5 cells/well), plates were incubated for 24 h, and cultures were treated for 72 h with CNPs or PBS. Then cells were trypsinized, washed three times with PBS, resuspended in binding buffer, and incubated with fluorescein isothiocyanate (FITC)-annexin V and propidium iodide (PI) in the dark for 15 min at normal temperature. Stained cells were immediately analyzed by fluorescence-activated cell sorting on a flow cytometer (BD Biosciences).

Autophagy detection

Ad-mRFP-GFP-LC3 adenovirus, which carries genes encoding modified red fluorescent protein (mRFP) and green fluorescent protein (GFP), HK-2 cells were transfected with Ad-mRFP-GFP-LC3 adenovirus according to the manufacturer's instructions (Hanbio Biotechnology, Shanghai, China). After

treatment with PBS or CNPs 12 h, cells were analyzed by confocal microscopy loss of green color and increase red spots to indicate fusion of lysosomes and autophagosomes and appearance of yellow color spots (merge of red and green) to indicate formation of autolysosomes.

Effects of CNPs on cell morphology and CNPs in specimens

HK-2 cells in 6-well plates were exposed for 12 or 72 h to CNPs (2 MCF). Cell morphology, internal structure, and intracellular localization of CNPs were analyzed using transmission electron microscopy. 20 specimens of the renal papillary calcified tissue from kidney stone patient were obtained in surgery, the localization of CNPs were analyzed using transmission electron microscopy.

Western blotting

HK-2 cells were plated in 6-well dishes, cultured for 24 h, then treated with CNPs (2 MCF) for 0, 12 and 72 h. The culture medium was aspirated and cells were washed three times with ice-cold PBS, then trypsinized and lysed with RIPA lysis solution (100 µl/well) for 30 min at 4 °C. Equal amounts of total cell lysates were subjected to Western blotting using rabbit monoclonal antibodies against Bax, Bcl-2, Beclin-1, LC3-B, JNK, p-JNK, p38 MAPK, p-p38 MAPK and GAPDH (Cell Signaling Technology, USA), Anti-fetuin-A antibody (EPR9291) was bought from abcam, All of the antibodies were diluted to 1:1000.

Ethics statement

The study protocol was approved by the Ethics Committee of Guangxi Medical University (Guangxi, China). Written informed consent was obtained from all subjects, who were treated in accordance with the Declaration of Helsinki.

Statistical analysis

Results are shown as mean ± SD and were analyzed using SPSS 16.0 (IBM, Chicago, IL, USA). Differences between two groups were assessed for significance using Student's *t* test; differences among more than two groups were assessed using one-way ANOVA. The threshold of significance was defined as $^{*}P<0.05$, $^{**}P<0.01$.

Results

CNP characteristics (Fig. 1)

Electron microscopy of CNPs cultured for 6 weeks showed the classical elliptical–spherical morphology with a dense, needle-like hydroxyapatite shell (Fig. 1b, c). CNPs dividing by binary fission were observed [14] (Fig. 1a).The size range of CNPs were 15–500 nm, most particles ranged in diameter from 50 to 500 nm. The particles (Fig. 1d), which had negative zeta potential (Fig. 1e, f), contained primarily C, O, Ca and P (Fig. 1e–i). They also contained fetuin-A, based on Western blotting (Fig. 1j).

CNP cytotoxicity

Exposing HK-2 cells for 72 h to CNPs significantly reduced viability ($P<0.01$, Fig. 2). In contrast, viability was similar in cultures exposed to CNPs for 12 h and 0 h ($P>0.05$).

CNPs in calcified plaque of renal papilla

Microscopy revealed similar morphology of CNPs from midstream urine of patients with kidney stones (Fig. 3a), CNPs in HK-2 cells (Fig. 3b), and CNPs in calcified plaques of renal papilla (Fig. 3c).

ROS induction by CNPs

ROS production was significantly higher in HK-2 cells exposed to CNPs for 72 h than in cells exposed to CNPs for 0 h ($^{**}P<0.01$) and in cells exposed to CNPs for 12 h ($^{**}P<0.01$) (Fig. 4).

CNP-induced changes in mitochondrial membrane potential

Mitochondrial membrane potential was significantly lower in HK-2 cells exposed to CNPs for 72 h than in cells exposed to CNPs for 0 h or cells exposed to CNPs for 12 h ($^{**}P<0.01$, Fig. 5).

Apoptosis induction by CNPs

Flow cytometric detection of double staining with annexin V-FITC and propidium iodide (PI) allows accurate detection of apoptosis. The percentage of apoptotic cells (Right upper quadrant add right lower quadrant) was significantly higher in HK-2 cells exposed to CNPs for 72 h than in cells exposed to PBS for 72 h ($P<0.01$, Fig. 6). Apoptotic

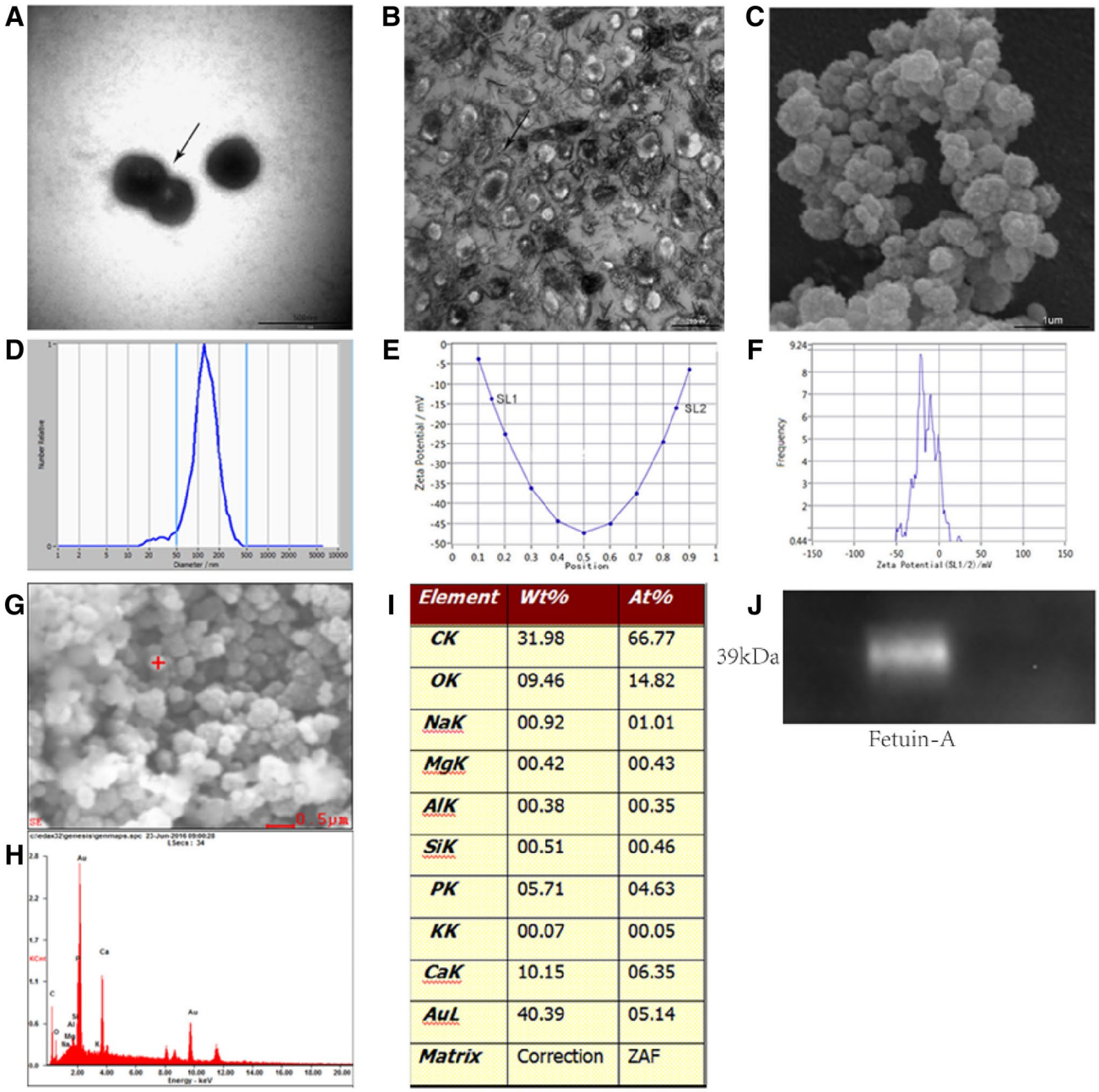

Element	Wt%	At%
CK	31.98	66.77
OK	09.46	14.82
NaK	00.92	01.01
MgK	00.42	00.43
AlK	00.38	00.35
SiK	00.51	00.46
PK	05.71	04.63
KK	00.07	00.05
CaK	10.15	06.35
AuL	40.39	05.14
Matrix	Correction	ZAF

Fig. 1 CNP characterization. **a** Transmission electron micrographs of CNPs from midstream urine of patients with kidney stones. **b** Transmission electron micrographs of CNPs following embedding. **c** Scanning electron micrographs of CNPs. **d–f** Electrophoresis and Brownian motion video analysis of CNP size, frequency and zeta potential. **g–i** Elemental composition of CNPs based on energy-dispersive X-ray microanalysis. **j** Positive result of Western blotting indicating the presence of fetuin-A in CNPs

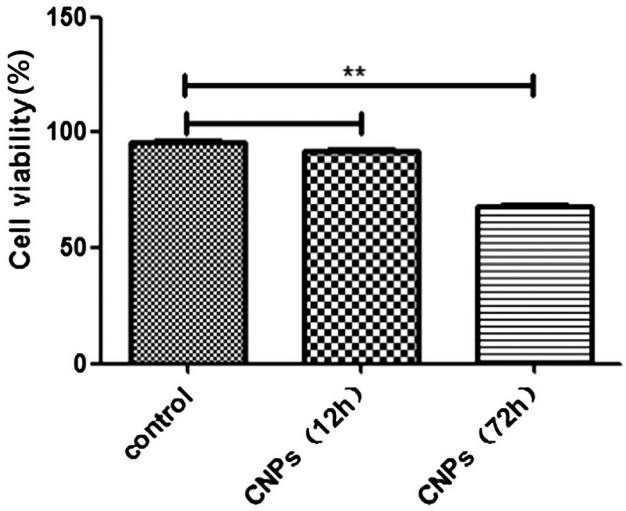

Fig. 2 Viability of HK-2 cells after exposure to CNPs for 0 h or to CNPs for 12 or 72 h. $^{**}P < 0.01$

cells in cultures exposed to CNPs contained cells in early apoptosis (annexin V-positive, PI-negative) as well as late apoptosis (annexin V-positive, PI-positive).

Autophagy induction by CNPs

HK-2 cells exposed to CNPs for 12 h contained significantly more yellow and red spots in the overlay image than cells exposed to PBS for 12 h, reflecting significantly more autophagosomes and autolysosomes ($P < 0.01$, Fig. 7).

Analysis of CNPs internalized by HK-2 cells

HK-2 cells internalized CNPs (Fig. 8a), and the morphology of intracellular CNPs based on transmission electron microscopy was similar to that of cultured CNPs isolated from patients. Intracellular CNP aggregates were observed (Fig. 8b, c), as well as mitochondrial swelling, vacuolization, and accumulation of CNPs inside intracellular vesicles (Fig. 8d–e). Characteristic features of apoptosis (Fig. 8i, Apoptotic body), autophagy (Fig. 8h, Autophagy or autophagic lysosome) and necrosis (Nuclear fragmentation or nuclear dissolution) were observed (Fig. 8f, g).

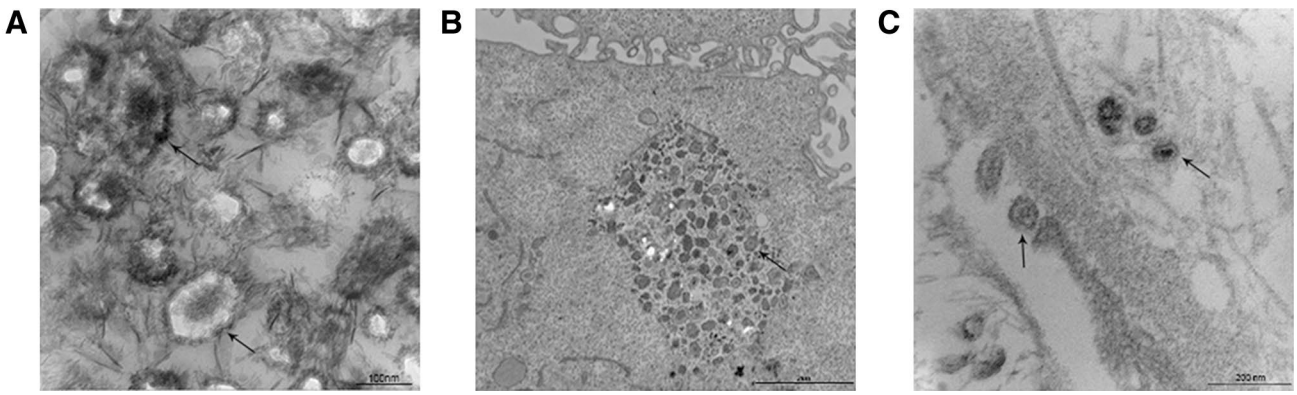

Fig. 3 Transmission electron micrographs of CNPs in **a** ultrathin sections of CNPs, **b** HK-2 cells and **c** calcified plaques in renal papilla from a patient

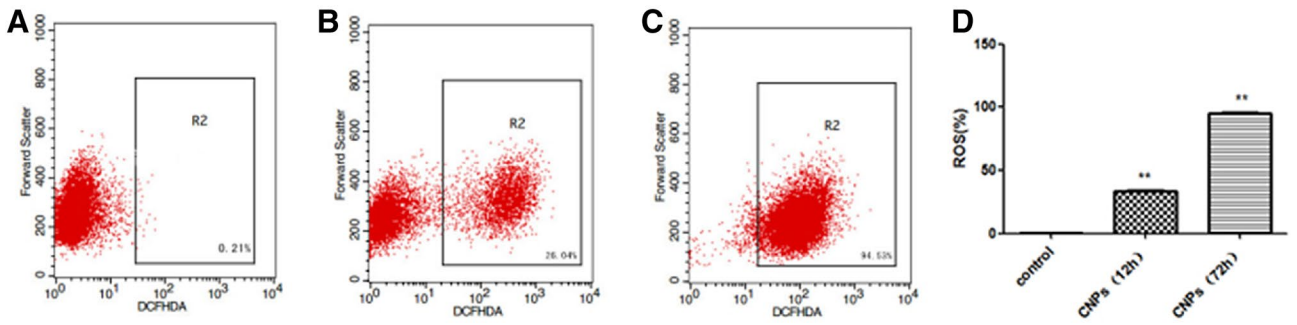

Fig. 4 ROS production in HK-2 cells exposed to **a** CNPs for 0 h, **b** CNPs for 12 h or **c** CNPs for 72 h. **d** Quantitation of flow cytometry data. $^{**}P < 0.01$

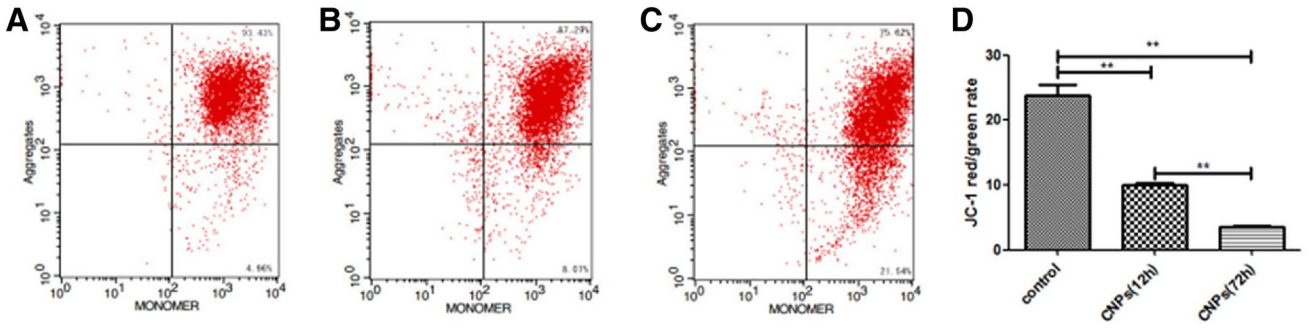

Fig. 5 Change in mitochondrial membrane potential in HK-2 cells after exposure to **a** CNPs for 0 h, **b** CNPs for 12 h, or **c** CNPs for 72 h. **d** Quantitation of flow cytometry data. $^{**}P < 0.01$

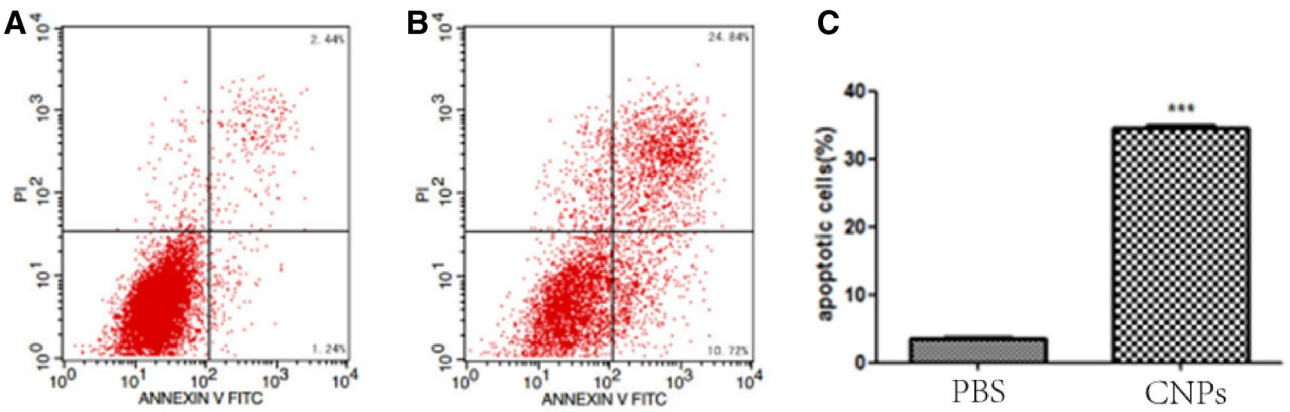

Fig. 6 Levels of apoptosis in HK-2 cells based on double staining with annexin V-FITC and propidium iodide (PI) following exposure to **a** PBS- for 72 h or **b** CNPs for 72 h. **c** Quantitation of flow cytometry data. $^{***}P < 0.001$

CNP-induced changes in protein expression

Exposing HK-2 cells for 12 h to CNPs significantly up-regulated expression of proteins LC3-II, Beclin-1 which represent autophagy markersand the apoptosis indicator protein Bax ($P < 0.01$, Fig. 9). Conversely, negative indicator of apoptosis Bcl-2 protein was significantly down-regulated ($P < 0.01$). The ratios of p-JNK to total JNK (second band) after 12-h exposure to CNPs was significantly higher than after exposure to CNPs for 0 h ($P < 0.01$), but of p-p38 MAPK to total p38 MAPK was not ($P > 0.05$). In addition, the ratio of p-JNK to total JNK was significantly higher after 12-h exposure than after 72-h exposure ($P < 0.01$).

Discussion

Urolithiasis is one of the most common urologic diseases worldwide, affecting up to 20% of adults in developed nations [15]. The primary origin of upper urinary calculi is kidney stones, the formation of which is poorly understood. Several theories have attempted to account for the formation of renal calculi as a result of inflammation, saturation, and crystal cell reactions. According to one of the more widely advocated theories, kidney stones form initially at Randall's plaque sites at or near the papillary tip in kidneys [4, 16, 17]. CNPs [14], which are ubiquitous particles found in soil, water and air [18], may play a role in kidney stone formation. Therefore, we examined the effects of CNPs on kidney epithelial cells.

When we cultured CNPs from midstream urine of patients with calcium oxalate stones, we found their morphology and internal structure to be consistent with the classical description [19, 20]. We observed the same structure in renal papilla calcifications of such patients using transmission electron microscopy, consistent with previous work [9]. These results are consistent with the hypothesis that CNPs contribute to kidney stone formation. Next we examined the effects of CNPs on HK-2 human kidney epithelial cells to identify possible pathway(s) and process(es) by which CNPs may drive kidney stone formation. We found that CNPs induced autophagy, apoptosis, and signaling mediated by ROS and JNK. These findings point to potential pathways of kidney stone formation that should be investigated in detail in future

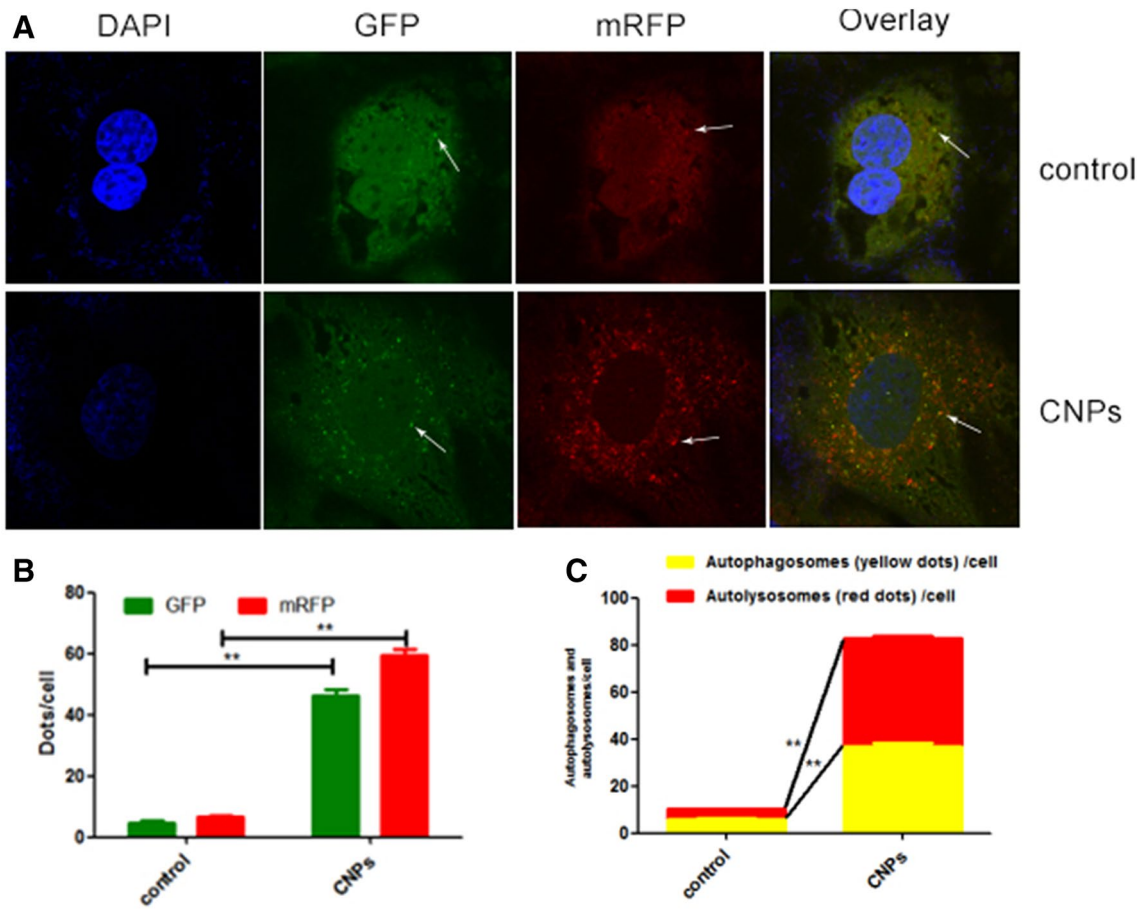

Fig. 7 Autophagy induction by CNPs.HK-2 cells were exposed (or not) to CNPs, then transduced with Ad-mRFP-GFP-LC3 adenovirus. **a** Red dots (mRFP) correspond to LC3. Yellow dots in the overlay image indicate autophagosomes, while red dots in the overlay image correspond to autolysosomes. **b** Quantitation of green and red dots per cell. **c** Quantitation of autophagosomes and autolysosomes per cell. Results are mean ± SD of at least 5 independent experiments. $^{**}P < 0.01$

work. Our electron microscopy studies of HK-2 cells that internalized CNPs revealed the presence of intracellular CNP aggregates and CNPs within vesicles. These results suggest that HK-2 may play an important role in CNP transport, which may depend on the negative zeta potential of CNPs. This transport may be mediated, at least in part, by endocytosis of CNPs. Future work should examine mechanisms of CNP transport in greater detail.

Most CNPs that we cultured from urine were smaller than 200 nm (Fig. 1), which were probably small enough to pass through the aperture barrier of the glomerular filtration membrane, enter the pro-urine and deposit in the renal papilla. Previous work has shown that CNPs tend to accumulate in the kidney [21]. Energy-dispersive X-ray microanalysis revealed the primary components of our cultured CNPs to be calcium and phosphorus. This is consistent with data indicating that the main component of Randall's plaques is calcium phosphate, not calcium oxalate [22], and that calcium phosphate forms the core of calcium oxalate stones [23–25]. Our Western blotting confirmed the presence of fetuin-A in cultured CNPs, consistent with previous reports that fetal globulin is abundant in CNPs [26] and that fetuin-A is the key material of CNP replication [27].

Numerous studies suggest that crystal-induced damage to renal tubular epithelial cells, collecting tubules and renal papillae helps drive kidney stone formation [28]. Our experiments identify several mechanisms by which CNPs may cause such damage, including induction of ROS production, autophagy and apoptosis. Exposing HK-2 cells to CNPs led to swelling and vacuolization of mitochondria around CNPs, and it decreased mitochondrial membrane potential, indicating mitochondrial damage. Mitochondrial dysfunction leads to intracellular ROS overload, which can further damage mitochondria as well as other cellular components. Probably in response to increased ROS production, we observed signs of autophagy based on electron microscopy, immunofluorescence and Western blotting of LC3 and Beclin-1 levels. In autophagy, cells can degrade cytoplasmic proteins and

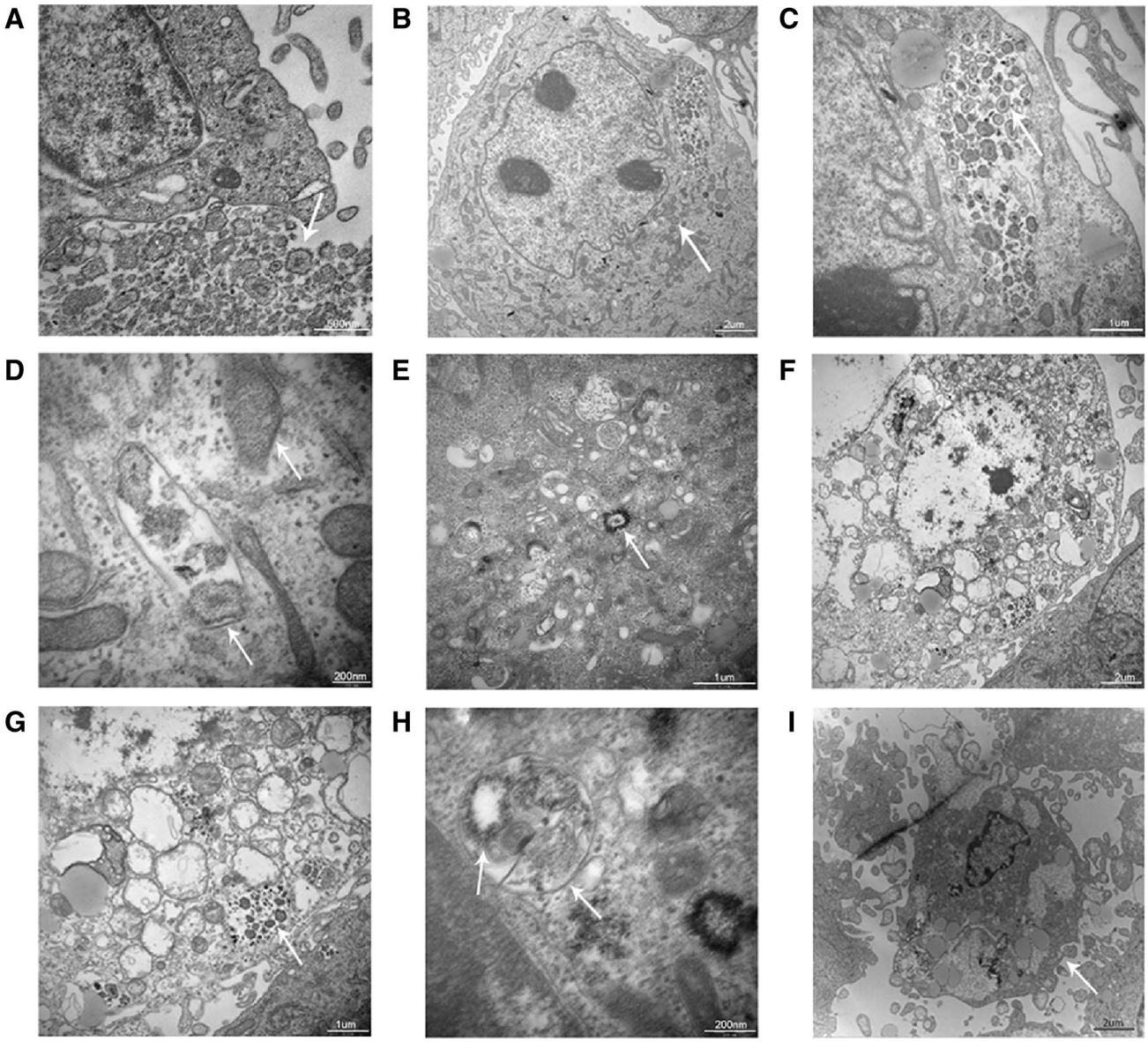

Fig. 8 Transmission electron micrographs of HK-2 cells exposed to CNPs, illustrating different aspects of CNP-induced damage. **a** CNPs entered cells via phagocytosis. Arrow, CNP. **b** Intracellular CNPs as well as swollen mitochondria (arrow). **c** Zoom-in of panel B. **d** Swollen mitochondria and CNPs within a vesicle (arrow). **e** CNP (arrow) within a cell showing swelling and vacuolization of nearby mitochondria. **f** CNPs in cells showing signs of cytolysis. **g** Zoom-in of panel **f**. The arrow indicates CNPs. **h** Autophagy of CNPs and organelles. **i** Apoptotic cell (arrow)

organelles via a lysosomal pathway [29]. The CNP-induced effects on ROS production, mitochondrial membrane potential and autophagy worsened with time, based on our analysis after 12 and 72 h of CNP exposure.

Our results highlight the potential importance of ROS in kidney stone formation. They are consistent with a model in which CNPs induce ROS production, which cells attempt to compensate for by up-regulating autophagy via activation of the MAP kinase JNK. This is consistent with previous reports identifying JNK as regulated by ROS [30]. Interestingly, although we observed increased levels of p-JNK after CNP exposure, we did not see an obvious increase in p-p38 MAPK levels, even though both p38 MAPK and JNK belong to the same family of serine/threonine kinases that regulate various cellular events such as proliferation and apoptosis [31]. This suggests that future studies of the potential role of ROS in kidney stone formation may wish to focus on JNK rather than p38 MAPK.

While the up-regulation of autophagy observed with CNP exposure may initially serve to reduce the increased production of ROS, the accumulation of ROS over longer CNP exposure may lead autophagy and apoptosis pathways

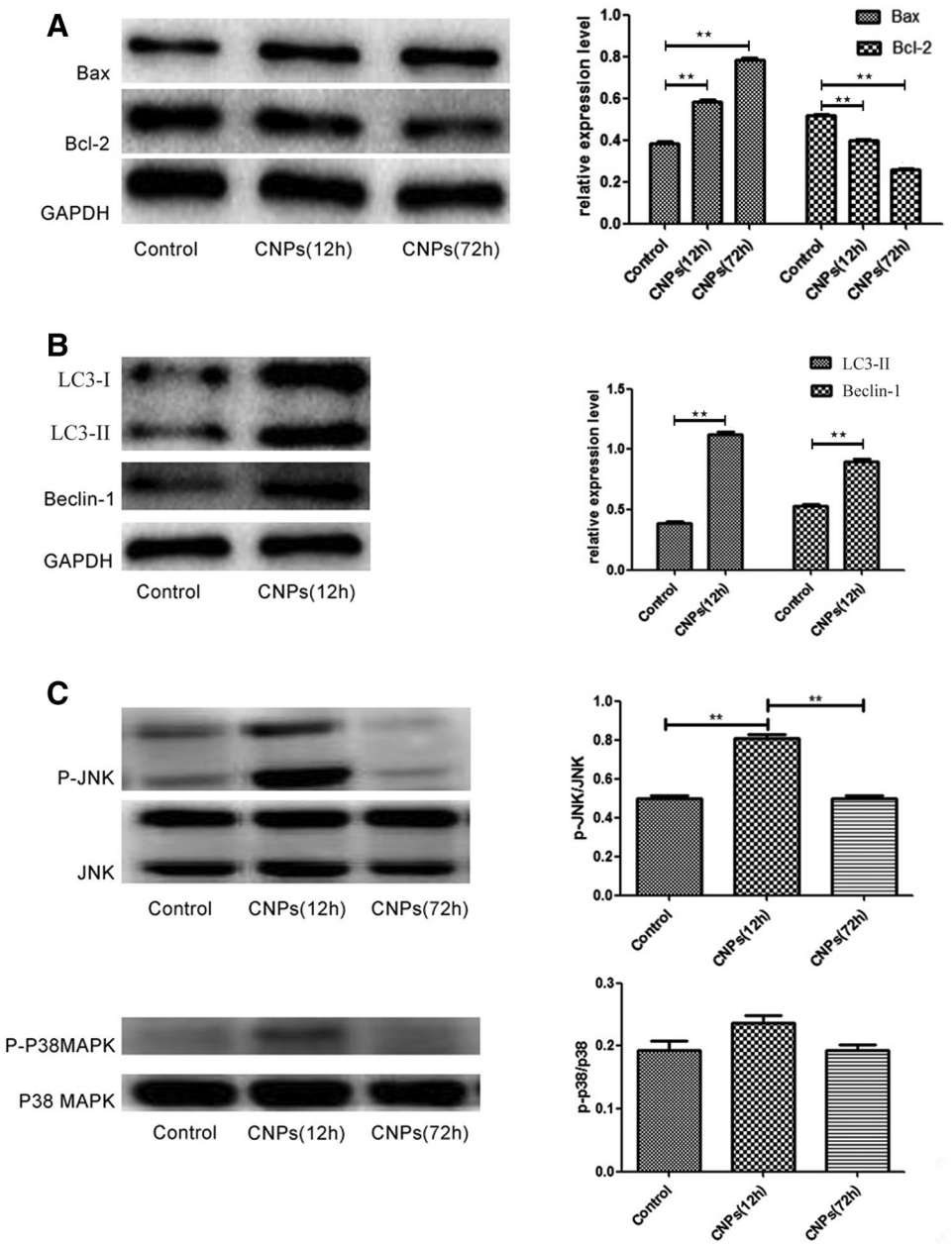

Fig. 9 Expression of various proteins in HK-2 cells exposed to CNPs for 0 h, CNPs for 12 h or CNPs for 72 h.Left panels show Western blot results; right panels show the corresponding quantitation. $^{**}P < 0.01$

to converge towards destroying CNP-affected cells. Previous work has shown that autophagy can reinforce apoptotic pathways [32] or work against them [33], depending on the degree of cell injury or ROS level in the cell [34–36]. The complex relationship between these two processes is mediated by common signaling molecules such as JNK and Akt. JNK, for example, activates the autophagy protein Beclin-1 as well as the apoptotic protein Bcl-2 [37, 38]. Activated JNK stimulates ROS production via a Bax-caspase-3 pathway, and the resulting ROS further activate JNK, leading ultimately to cell death [39]. Future work should clarify the different roles of autophagy and apoptosis in CNP-induced kidney epithelial injury, and explore how this injury may drive kidney stone formation.

We speculate that CNP-induced apoptosis and related necrosis, which we observed here using flow cytometry and transmission electron microscopy, can lead to local inflammation and aggravate initial damage. Degraded protein and other nutrients from necrotic cells may provide raw material for CNP proliferation. Building blocks for CNPs may come also from urinary components such as fetuin-A. These processes may then give rise to Randall's plaque formation. This model should be tested in future work.

Funding This work was supported by grants from the National Natural Science Foundation of China (No. 81760127, 81360113, 30860280 and 30960455), the Guangxi Natural Science Foundation (No. 2017GXNSFAA198070). We are grateful to the members of the Electron Microscopy Group in the Department of Life Science at Guangxi Medical University, Guangxi, and People's Republic of China.

Compliance with ethical standards

Conflict of interest All authors declare that they have no any conflict of interests.

Ethical approval The study protocol was approved by the Ethics Committee of Guangxi Medical University (Guangxi, China).

Informed consent Informed consent was obtained from all individual participants included in the study.

References

1. Wang WJ, Fan JY, Huang GF, Li J, Zhu X, Tian Y, Su L(2017) Prevalence of kidney stones in mainland China: a systematic review. Sci Rep 7:41630
2. Romero V, Akpinar H, Assimos DG (2010) Kidney stones: a global picture of prevalence, incidence, and associated risk factors. Rev Urol 12:e86–e96
3. Sutherland JW, Parks JH, Coe FL (1985) Recurrence after a single renal stone in a community practice. Miner Electrolyte Metab 11(4):267–269
4. Randall A (1937) The origin and growth of renal calculi. Ann Surg 105(6):1009–1027
5. Çiftçioglu N, Kajander EO (1998) Interaction of nanobacteria with cultured mammalian cells. Pathophysiology 4:259–270
6. Cisar JO, Xu DQ, Thompson J, Swaim W, Hu L, Dennis J (2000) An alternative interpretation of nanobacteria-induced biomineralization. PNAS 97(21):11511–11515
7. Miller VM, Rodgers G, Charlesworth JA, Kirkland B, Severson SR, Rasmussen TE, Yagubyan M, Rodgers JC, Cockerill FR 3rd, Folk RL, Rzewuska-Lech E, Kumar V, Farell-Baril G, Lieske JC (2004) Evidence of nanobacterial-like structures in calcified human arteries and cardiac valves. Am J Physiol Heart Circ Physiol 287(3):H1115–24. https://doi.org/10.1152/ajpheart.00075.2004
8. Martel J, Peng HH, Young D, Wu CY, Young JD (2014) Of nanobacteria, nanoparticles, biofilms and their role in health and disease: facts, fancy and future. Nanomedicine 9(4):483–499
9. Ciftcioglu N, Vejdani K, Lee O, Mathew G, Aho KM, Kajander EO, McKay DS, Jones JA, Stoller ML (2008) Association between Randall's plaque and calcifying nanoparticles. Int J Nanomed 3(1):105–115
10. Zhang MJ, Liu SN, Xu G, Guo YN, Fu JN, Zhang DC (2014) Cytotoxicity and apoptosis induced by nanobacteria in human breast cancer cells. Int J Nanomed 9:265–271. https://doi.org/10.2147/IJN.S54906
11. Zhang M, Yang J, Shu J, Fu C, Liu S, Xu G, Zhang D (2014) Cytotoxicity induced by nanobacteria and nanohydroxyapatites in human choriocarcinoma cells. Nanoscale Res Lett 9(1):616. https://doi.org/10.1186/1556-276X-9-616
12. Wong T-Y, Wu C-Y, Martel J (2015) Detection and characterization of mineralo-organic nanoparticles in human kidneys. Sci Rep 5:15272
13. Miller C, Kennington L, Cooney R, Kohjimoto Y, Cao LC, Honeyman T, Pullman J, Jonassen J, Scheid C (2000) Oxalate toxicity in renal epithelial cells: characteristics of apoptosis and necrosis. Toxicol Appl Pharmacol 162(2):132–141. https://doi.org/10.1006/taap.1999.8835
14. Kajander EO, Kuronen I, Akerman KK (1997) Nanobacteria from blood: the smallest culturable autonomously replicating agent on earth. SPIE Proc 3111:420–428
15. Trinchieri A (1996) Epidemiology of urolithiasis. Arch Ital Urol Androl 68(4):203–249
16. Evan AP, Lingeman JE, Coe FL, Parks JH, Bledsoe SB (2003) Randall's plaque of patients with nephrolithiasis begins in basement membranes of thin loops of Henle. J Clin Investig 111(5):607–616. https://doi.org/10.1172/JCI200317038
17. Evan AP (2010) Physiopathology and etiology of stone formation in the kidney and the urinary tract. Pediatr Nephrol 25(5):831–841
18. Smirnov GV, Smirnov DG (2008) Nannobacteria: a new ecological threat. Contemp Probl Ecol 1:111–114
19. Kajander EO, Ciftcioglu N (1998) Nanobacteria: an alternative mechanism for pathogenic intra- and extracellular calcification and stone formation. Proc Natl Acad Sci USA 95(14):8274–8279
20. Kajander EO, Ciftcioglu N, Aho K, Garcia-Cuerpo E (2003) Characteristics of nanobacteria and their possible role in stone formation. Urol Res 31(2):47–54. https://doi.org/10.1007/s00240-003-0304-7
21. Akerman KK, Kuikka JT, Cificioglu N (1997) Radio labeling and in vivo distribution of nanobacteria in rabbit. Proc SPIE 13:436–442
22. Coe FL, Evan A, Worcester E (2005) Kidney stone disease. J Clin Invest 115(10):2598–2608. https://doi.org/10.1172/JCI26662
23. Grases F, March JG, Conte A, Costa-Bauza A (1993) New aspects on the composition, structure and origin of calcium oxalate monohydrate calculi. Eur Urol 24(3):381–386
24. Abraham PA, Smith CL (1987) Evaluation of factors involved in calcium stone formation. Miner Electrolyte Metab 13(3):201–208
25. Ciftcioglu N, Haddad RS, Golden DC, Morrison DR, McKay DS (2005) A potential cause for kidney stone formation during space flights: enhanced growth of nanobacteria in microgravity. Kidney Int 67(2):483–491. https://doi.org/10.1111/j.1523-1755.2005.67105.x
26. Raoult D, Drancourt M, Azza S, Nappez C, Guieu R, Rolain JM, Fourquet P, Campagna B, La Scola B, Mege JL, Mansuelle P, Lechevalier E, Berland Y, Gorvel JP, Renesto P (2008) Nanobacteria are mineralo fetuin complexes. PLoS Pathog 4(2):e41. https://doi.org/10.1371/journal.ppat.0040041
27. Chabriere E, Gonzalez D, Azza S, Durand P, Shiekh FA, Moal V, Baudoin JP, Pagnier I, Raoult D (2014) Fetuin is the key for nanon self-propagation. Microb Pathog 73:25–30. https://doi.org/10.1016/j.micpath.2014.05.003
28. Verkoelen CF, van der Boom BG, Houtsmuller AB, Schroder FH, Romijn JC (1998) Increased calcium oxalate monohydrate crystal binding to injured renal tubular epithelial cells in culture. Am J Physiol 274(5 Pt 2):F958–965
29. Choi AM, Ryter SW, Levine B (2013) Autophagy in human health and disease. N Engl J Med 368(7):651–662. https://doi.org/10.1056/NEJMra1205406
30. Scherz-Shouval R, Elazar Z (2011) Regulation of autophagy by ROS: physiology and pathology. Trends Biochem Sci 36(1):30–38. https://doi.org/10.1016/j.tibs.2010.07.007
31. Ki YW, Park JH, Lee JE, Shin IC, Koh HC (2013) JNK and p38 MAPK regulate oxidative stress and the inflammatory response in chlorpyrifos-induced apoptosis. Toxicol Lett 218(3):235–245. https://doi.org/10.1016/j.toxlet.2013.02.003
32. Salazar M, Carracedo A, Salanueva IJ, Hernandez-Tiedra S, Lorente M, Egia A, Vazquez P, Blazquez C, Torres S, Garcia S, Nowak J, Fimia GM, Piacentini M, Cecconi F, Pandolfi PP,

Gonzalez-Feria L, Iovanna JL, Guzman M, Boya P, Velasco G (2009) Cannabinoid action induces autophagy-mediated cell death through stimulation of ER stress in human glioma cells. J Clin Invest 119(5):1359–1372

33. Pan X, Zhang X, Sun H, Zhang J, Yan M, Zhang H (2013) Autophagy inhibition promotes 5-fluorouraci-induced apoptosis by stimulating ROS formation in human non-small cell lung cancer A549 cells. PLoS One 8(2):e56679. https://doi.org/10.1371/journal.pone.0056679
34. Eisenberg-Lerner A, Bialik S, Simon HU, Kimchi A (2009) Life and death partners: apoptosis, autophagy and the cross-talk between them. Cell Death Differ 16(7):966–975. https://doi.org/10.1038/cdd.2009.33
35. Nikoletopoulou V, Markaki M, Palikaras K, Tavernarakis N (2013) Crosstalk between apoptosis, necrosis and autophagy. Biochim Biophys Acta 1833(12):3448–3459. https://doi.org/10.1016/j.bbamcr.2013.06.001
36. Moretti L, Cha YI, Niermann KJ, Lu B (2007) Switch between apoptosis and autophagy: radiation-induced endoplasmic reticulum stress? Cell Cycle 6(7):793–798. https://doi.org/10.4161/cc.6.7.4036
37. Wong CH, Iskandar KB, Yadav SK, Hirpara JL, Loh T, Pervaiz S (2010) Simultaneous induction of non-canonical autophagy and apoptosis in cancer cells by ROS-dependent ERK and JNK activation. PLoS One 5(4):e9996. https://doi.org/10.1371/journal.pone.0009996
38. Wei Y, Pattingre S, Sinha S, Bassik M, Levine B (2008) JNK1-mediated phosphorylation of Bcl-2 regulates starvation-induced autophagy. Mol Cell 30(6):678–688. https://doi.org/10.1016/j.molcel.2008.06.001
39. Kim EM, Yang HS, Kang SW, Ho JN, Lee SB, Um HD (2008) Amplification of the gamma-irradiation-induced cell death pathway by reactive oxygen species in human U937 cells. Cell Signal 20(5):916–924. https://doi.org/10.1016/j.cellsig.2008.01.002